

Human circular RNA-0054633 regulates high glucose-induced vascular endothelial cell dysfunction through the microRNA-218/roundabout 1 and microRNA-218/heme oxygenase-1 axes

LONG PAN^{1,2*}, WEISHUAI LIAN^{1,2*}, XIAOJUN ZHANG^{1,2}, SHILONG HAN^{1,2}, CHUANWU CAO^{1,2},
XUE LI^{1,2} and MAOQUAN LI^{1,2}

¹Department of Interventional and Vascular Surgery, Tenth People's Hospital of Tongji University;

²Institute of Interventional and Vascular Surgery, Tongji University, Shanghai 200072, P.R. China

Received September 29, 2017; Accepted March 27, 2018

DOI: 10.3892/ijmm.2018.3625

Abstract. The aim of the present study was to investigate the relative regulation of human circular RNA-0054633 (hsa_circ_0054633), microRNA-218 (miR-218), roundabout 1 (ROBO1) and heme oxygenase-1 (HO-1) in human umbilical vein endothelial cells (HUVECs) in high glucose conditions. Initially, the expression of hsa_circ_0054633 in HUVECs was detected in high glucose conditions by reverse transcription-quantitative polymerase chain reaction. Next, a small interfering RNA against hsa_circ_0054633 was constructed to investigate the function of hsa_circ_0054633 in HUVECs by transwell migration, cell counting kit-8, flow cytometry and tube formation assays. In addition, the effect of hsa_circ_0054633 on the expression levels of ROBO1, HO-1 and vascular endothelial growth factor were examined. The regulation effects of hsa_circ_0054633 on high glucose-induced HUVEC proliferation, migration, and angiogenesis were also analyzed. Bioinformatics analysis and dual-luciferase assay were then used to confirm the direct or specific regulation of hsa_circ_0054633, miR-218, ROBO1 and HO-1. It was observed that high glucose levels increased the expression of hsa_circ_0054633, while downregulation of hsa_circRNA-0054633 increased the high glucose-induced endothelial cell dysfunction, including proliferation, migration

and angiogenesis suppression. Bioinformatics analysis revealed that the expression of circRNA-0054633 was able to inhibit miR-218 expression, which was clarified by the dual-luciferase assay. It was also demonstrated that downregulating the expression of miR-218 inhibited the high glucose-induced endothelial cell dysfunction by promoting the expression of ROBO1 and HO-1. These results suggest that the expression of hsa_circRNA-0054633 has a protective effect against high glucose-induced endothelial cell dysfunction by targeting ROBO1 and HO-1.

Introduction

Diabetes mellitus (DM) is a metabolic disorder that constitutes a major global health problem (1). It has been estimated that by 2030, significant alterations in the nutrition and lifestyle in developing countries within Asia and the Middle East will lead to a marked increase in the prevalence of type 2 DM (T2DM) worldwide (2,3). Cardiovascular disease (CVD) is the leading cause of morbidity and mortality as a result of diabetes, accounting for up to 80% of premature mortality cases in diabetes patients (4,5). Endothelial damage is critical in the development of CVD, and the inhibition of endothelial cell migration and angiogenesis are limiting processes in the repair of the endothelium (6,7). However, the mechanism of endothelial damage is currently unclear.

Increasing evidence has verified that non-coding RNAs serve an important role in the regulation of cell metabolism (8,9). Circular RNAs (circRNAs) are a subclass of endogenous non-coding RNAs, mainly consisting of exonic transcripts generated through the process of back-splicing (10). Recently, it has been reported that circRNAs are widely expressed in human cells and function as vital regulators in the process of transcriptional and post-transcriptional gene expression (11). Zhao *et al* (12) observed that the expression of hsa_circ_0054633 was significantly increased in T2DM. Therefore, hsa_circ_0054633 presents a potential diagnostic ability for pre-diabetes and T2DM. However, the regulating effect of hsa_circ_0054633 in diabetes remains unclear.

Correspondence to: Dr Maoquan Li or Dr Xue Li, Department of Interventional and Vascular Surgery, Tenth People's Hospital of Tongji University, 301 Middle Yan Chang Road, Shanghai 200072, P.R. China
E-mail: cjr.limaquan@vip.163.com
E-mail: lixue5303@126.com

*Contributed equally

Key words: hsa_circ_0054633, microRNA-218, roundabout 1, heme oxygenase-1, high glucose

In diabetes, the roles of long non-coding RNA (lncRNA) and microRNA (miRNA) have been systematically expanded (13). Our previous studies revealed that the lncRNA MALAT1 regulates renal tubular epithelial pyroptosis by modulating the miR-23c that targets ELAVL1 in diabetic nephropathy (14). circRNAs that have yet to be extensively studied may constitute a novel reservoir of therapeutic targets and biomarkers (15). It has been reported that circRNAs are miRNA sponges, which may serve as a novel class of biomarkers in diabetes (16). Yang *et al* (17) identified that miR-218 was upregulated in podocytes treated with a high glucose concentration and promoted high glucose-induced apoptosis in these cells by targeting heme oxygenase-1 (HO-1). Zhang *et al* (18) also observed that miR-218 expression promoted angiogenesis by targeting roundabout 1 (ROBO1). ROBO1, also known as protein SAX3, is the receptor of slit guidance ligand 1 (SLIT1) and SLIT2, which are associated with cell migration. In addition, several studies have demonstrated that ROBO1 functions as a promoter of cell proliferation (19). It has also been observed that the expression of miR-218 has an inhibitory effect on cell proliferation and metastasis (19,20). These previous findings suggested that the expression of miR-218 suppressed cell proliferation and metastasis by targeting ROBO1. Furthermore, a previous study identified that miR-218 accelerated high glucose-induced podocyte apoptosis through directly down-regulating HO-1 (17). HO-1, an antioxidant and cytoprotective enzyme, has been reported to have a protective effect against high glucose-induced cell toxicity, including oxidative stress and inflammation. Additionally, the expression of HO-1 offered protection against high glucose-induced apoptosis in endothelial cells and promoted angiogenesis (21).

In the present study, bioinformatics analysis (circnet.mbc.ntu.edu.tw/) identified that hsa_circ_0054633 targets miR-218 and inhibits miR-218 expression. It was observed that the expression of hsa_circ_0054633 was able to regulate the high glucose-induced dysfunction including proliferation, migration and angiogenesis suppression in endothelial cells by targeting miR-218. It was also demonstrated that downregulating the expression of miR-218 inhibited the high glucose-induced endothelial cell dysfunction by relieving the targeting of ROBO1 and HO-1. Furthermore, hsa_circ_0054633 functions as an miR-218 sponge, leading to the subsequent upregulation of HO-1 and ROBO1.

Materials and methods

Cell culture and high glucose treatment. Human umbilical vein endothelial cells (HUVECs) were obtained from the American Type Culture Collection (Manassas, VA, USA) and cultured in Dulbecco's modified Eagle's medium (Invitrogen; Thermo Fisher Scientific, Inc., Waltham, MA, USA) supplemented with 10% fetal bovine serum (FBS; Sigma-Aldrich; Merck KGaA, Darmstadt, Germany) at 37°C in a humidified atmosphere containing 5% CO₂. For high sugar analysis, HUVECs were assigned to the normal glucose-treated (NG; 5.5 mmol/l; control) or high glucose-treated (HG; 33.3 mmol/l) groups, and the treatments were performed as previously reported (22). Following incubation for 48 h, HUVECs were trypsinized prior to collected by centrifugation (2,000 x g for

5 min) at room temperature, and then subjected to proliferation, migration and angiogenesis analyses.

Cell mimic transfection or inhibitor treatment. For miR-218 overexpression, miR-218 mimics or a corresponding miR-negative control (NC) were purchased from GenePharma Co., Ltd. (Shanghai, China). Next, HUVECs were transfected with miR-218 mimic or miR-NC at a final concentration of 50 nM using Lipofectamine® 2000 (Invitrogen; Thermo Fisher Scientific, Inc.) according to the manufacturer's protocol. For miR-218 expression inhibition, HUVECs was pretreated with 5 nM miR-218 inhibitor (Invitrogen; Thermo Fisher Scientific, Inc.). Following transfection with miR-218 mimics or treatment with miR-218 inhibitor, cells were incubated at 37°C with 5% CO₂ for 48 h, and then used for miR-218 expression analysis or other experiments. For hsa_circ_0054633 downregulation, small interfering RNA (siRNA) against hsa_circ_0054633 (5'-CCCAGAACAUAGACAAAUUUAU-3') or a NC (5'-GGGACUUCAGACAAAUUUAU-3') were constructed (GenePharma Co., Ltd.) and transfected into HUVECs for 48 h prior to further experiments.

Reverse transcription-quantitative polymerase chain reaction (RT-qPCR) analysis. Total RNA was isolated from cells using TRIzol reagent (Invitrogen; Thermo Fisher Scientific, Inc.) and the RNA concentration was determined by Multiskan Spectrum (Thermo Fisher Scientific, Inc.) at optical density 260/230. The RNA was then reverse transcribed into cDNA using the DyNAmo cDNA Synthesis kit (Pierce; Thermo Fisher Scientific, Inc.). qPCR was then performed on an HT7900 Real-Time PCR System (Applied Biosystems; Thermo Fisher Scientific, Inc.) using the following specific primers: Hsa_circ_0054633 (NM_021629.3) forward, 5'-CCAATATTGTATACTAGCTCCTC-3', and reverse, 5'-GCACTTTATTAGATTACAGTATC-3'; miR-218 (NR_029631.1) forward, 5'-GCGCTTGTGCTTGATCTAA-3', and reverse, 5'-GTGCAGGGTCCGAGGT-3'; U6 forward, 5'-CTCGCTTCGCGCAGCACA-3', and reverse, 5'-AACGCTTCACGAATTGCGT-3'; HO-1 (NC_000022.11) forward, 5'-CTCAAACCTCCAAAAGCC-3', and reverse, 5'-TCAAAAACCACCCCAACCC-3'; ROBO1 (NC_000003) forward, 5'-GGAAGAAGACGAAGCCGACAT-3', and reverse, 5'-TCTCCAGGTCCC CAACACTG-3'. PCR products were detected using the SYBR Green PCR Master Mix (Applied Biosystems; Thermo Fisher Scientific, Inc.). The thermocycling conditions were as follows: 95°C for 30 sec, followed by 40 cycles of 95°C for 30 sec, 60°C for 20 sec, 70°C for 1 min, with a final extension step at 70°C for 5 min. Relative mRNA levels were calculated following normalization to the U6 mRNA levels using the comparative cycle threshold ($2^{-\Delta\Delta C_q}$) method (23).

Flow cytometry. Flow cytometry was used to determine the rate of apoptosis in HUVECs. Apoptotic cells were differentiated from viable or necrotic cells by the combined application of Annexin V (AV)-FITC and propidium iodide (PI) (both Gibco; Thermo Fisher Scientific, Inc.). Briefly, cells were washed twice and adjusted to a concentration of 1×10^6 cells/ml with cold D-Hanks buffer (Gibco; Thermo Fisher Scientific, Inc.). Next, AV-FITC (10 μ l) and PI (10 μ l) were added to 100 μ l of cell suspension and incubated for 15 min at room temperature

in the dark. Finally, 400 μ l binding buffer was added to each sample without washing, and the samples were analyzed using flow cytometry. Each experiment was performed in triplicate.

Tube formation assay. *In vitro* neovascularization assays were performed in human fibrin matrices. Briefly, transfected HUVECs with/without sihsa_circ_0054633 were pretreated with different concentrations of glucose (5.5 or 33 mM) for 48 h and then plated (2×10^5 cells) on Matrigel. Next, serum-starved HUVECs (2×10^5 cells) were seeded onto 24-well plates coated with Matrigel (BD Biosciences, Franklin Lakes, NJ, USA) in endothelial basal medium and incubated at 37°C with 5% CO₂ for 16 h. Tubular structures of HUVECs in the Matrigel were analyzed by phase-contrast microscopy. To quantify the length of newly formed tubes, six random phase-contrast photomicrographs were captured per well.

Cell proliferation assays. The study next attempted to determine the effects of hsa_circ_0054633 on high glucose-induced HUVEC proliferation. Briefly, HUVECs transfected with/without siRNA against hsa_circ_0054633 or with/without high glucose treatment were seeded onto six 96-well plates at a density of 2×10^3 cells per well. Following incubation at 37°C with 5% CO₂ for 48 h, a cell counting kit-8 (CCK-8) assay (Dojindo Molecular Technologies, Inc., Kumamoto, Japan) was conducted according to the manufacturer's protocol. Briefly, DMEM (900 μ l) and CCK8 (100 μ l) were added to each well and incubated for 1.5 h at 37°C. Subsequently, the absorption of the cells was measured at a wavelength of 450 nm by an enzyme-linked immunosorbent assay reader (Thermo Fisher Scientific, Inc.). Data represent at least three independent experiments with three replications each time.

Boyden chamber assay. The migratory ability of HUVECs was evaluated with Transwell chambers (8 μ m; BD Biosciences). Briefly, cells suspended in 100 μ l medium without serum were seeded into the upper chamber at a density of $(5-10) \times 10^4$ cells/well, while the lower chamber was filled with 20% FBS to induce the migration or invasion of HUVECs through the membrane. For the invasion assay, Matrigel (1:6 dilution; BD Biosciences) was also added to the upper chamber. Subsequent to incubation at 37°C with 5% CO₂ for 24 h, cells that had migrated or invaded across the Transwell membrane were stained with crystal violet (MedChem Express, Shanghai, China) and counted under an optical microscope.

Western blot analysis. Total protein was extracted from the cells by lysis buffer (Gibco; Thermo Fisher Scientific, Inc.) containing protease inhibitors, and the cell lysate was centrifuged at $13,400 \times g$ at 4°C for 5 min. The protein concentration was then examined by a bicinchoninic acid kit (Pierce; Thermo Fisher Scientific, Inc.). Next, protein samples (40 μ g) were separated by SDS-polyacrylamide gel electrophoresis and transferred onto polyvinylidene difluoride membranes. Subsequent to blocking in 5% fat-free milk for 2 h at 4°C, the membranes were incubated at 4°C overnight with the following primary antibodies: Anti-ROBO1 (cat. no. sc-25672), anti-vascular endothelial growth factor (VEGF; cat. no. sc-4570), anti-HO-1 (cat. no. sc-120745)

and anti-GAPDH (cat. no. sc-293335) (all purchased from Santa Cruz Biotechnology, Inc., Dallas, TX, USA). All the antibodies were diluted to 1:1,000 with PBS prior to use. The membranes were then incubated for 1 h at room temperature with horseradish peroxidase-conjugated secondary antibodies (cat. no. sc-324565; Santa Cruz Biotechnology, Inc.). The blots were visualized using an Enhanced Chemiluminescence Detection kit obtained from GE Healthcare Life Sciences (Amersham; Little Chalfont, UK). The intensity of the protein bands was quantified with the Quantity One software 5.0 (Bio-Rad Laboratories, Inc., Hercules, CA, USA) and normalized against the loading controls.

Bioinformatics analysis. In order to identify the association among circRNA-0054633, miR-218, HO-1 and ROBO1, bioinformatics analysis (circnet.mbc.nctu.edu.tw/) was performed in the current study. The BioEdit 3.0 software (Ionis Pharmaceuticals, Inc., Carlsbad, CA, USA) was used for comparison of the interaction between miR-218 and circRNA. In addition, the database TargetScan (targetscan.org/) was used to search for potential interactions between miR-218 and the 3'-untranslated region (3'-UTR) of HO-1 or ROBO1.

Dual-luciferase reporter assay. A luciferase reporter assay was used to detect the direct binding of circRNA-0054633, miR-218, ROBO1 and HO-1. The firefly luciferase reporter assay was conducted using a pGL3 control vector (Promega Corporation, Madison, WI, USA). Initially, the wild-type and mutated 3'-UTR of ROBO1, wild-type and mutated 3'-UTR of HO-1 and wild-type and mutated circRNA-0054633 sequence containing putative miR-218 target sites or mutated 3'-UTR were constructed by replacing a number of binding sites of miR-218 with other nucleotides. These sequences were synthesized and subcloned into the pGL3 control vector. For the reporter assay, 0.1 mg pGL3 vectors containing wild-type or mutated 3'-UTR of HO-1 were co-transfected with pre-miR-218 or pre-miR-control into 293 cells (American Type Culture Collection) using Lipofectamine® 2000. Subsequent to transfection and incubation at 37°C with 5% CO₂ for 48 h, cells were harvested by centrifugation ($2,000 \times g$ for 5 min) at room temperature, and the luciferase activity was analyzed with the Dual-Luciferase Reporter Assay System (Promega Corporation).

Statistical analysis. Results are expressed as the mean \pm standard deviation. Statistically significant differences were evaluated by one-way analysis of variance followed by the Tukey's test. Groups were compared using GraphPad Prism software, version 5.0 (GraphPad Software, Inc., La Jolla, CA, USA). A value of $P < 0.05$ denotes a statistically significant difference.

Results

Regulation effect of circRNA-0054633 on high glucose-induced endothelial cell dysfunction. In a previous study, microarray analysis of the expression profiles of circRNAs in the peripheral blood of T2DM patients demonstrated that hsa_circ_0054633 was upregulated (12). However, the regulation mechanism remains unclear. Bioinformatics analysis

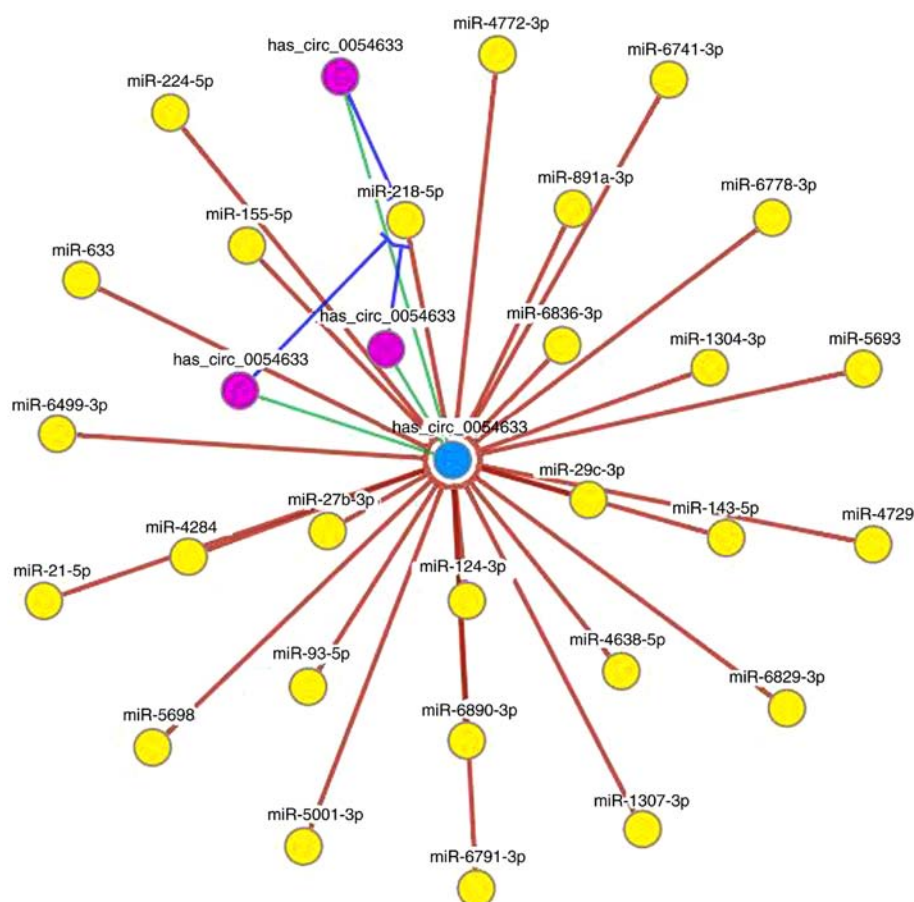


Figure 1. Bioinformatics analysis for hsa_circ_0054633. The purple points demonstrate that hsa_circ_0054633 interacts with miR-218. hsa_circ_0054633, human circular RNA-0054633; miR, microRNA.

identified that hsa_circ_0054633 targets miR-218 (Fig. 1). In this network, the circRNA/miRNA interaction was predicted, and the results revealed that miR-218 was one of the most likely predicted targets.

In order to identify the effect of hsa_circ_0054633 on endothelial cell proliferation, migration and angiopoiesis, siRNA against hsa_circ_0054633 was constructed or NC and transfected into HUVECs. In addition, to identify the effect of a high-glucose environment on the HUVECs, cells were also treated with different concentrations of glucose, namely 5.5 and 33 mmol/l, corresponding to the NG and HG groups. After 48 h of transfection, the expression of hsa_circ_0054633 was measured by RT-qPCR. The results revealed that the expression of hsa_circ_0054633 was significantly decreased in the siRNA-transfected cells compared with that in the NC-transfected cells in the NG and HG groups (Fig. 2A). Furthermore, high glucose treatment significantly increased the expression of hsa_circ_0054633 in the NC + HG cells, as compared with the NC + NG group. However, following transfection with siRNA against hsa_circ_0054633, the expression of hsa_circ_0054633 decreased significantly, even upon high glucose treatment (Fig. 2A).

The proliferation (Fig. 2B) and apoptosis (Fig. 2C and D) of HUVECs were detected by a CCK-8 assay. Flow cytometry demonstrated that in a HG environment (33 mM) the proliferative activity of HUVECs in the HG groups were

significantly inhibited (Fig. 2B), and the apoptotic ratio was markedly increased compared with the NG concentration (5.5 mM; Fig. 2C). In addition, downregulation of the expression of hsa_circ_0054633 further depressed the proliferative activity and increased the apoptotic ratio. Subsequently, the migration of HUVECs was detected by a Transwell assay. The results demonstrated that downregulation of the expression of hsa_circ_0054633 further depressed the high glucose-induced migration (Fig. 2E and F). To further assess the angiogenic function of hsa_circ_0054633, an *in vitro* capillary tube formation assay was employed in HUVECs. The results revealed that high glucose treatment significantly suppressed the tube formation, and this phenomenon was aggravated following the downregulation of hsa_circ_0054633 expression (Fig. 2G and H). Furthermore, western blot analysis was conducted and demonstrated that high glucose treatment increased the expression levels of ROBO1 and VEGF. However, the downregulation of hsa_circ_0054633 expression significantly decreased the ROBO1 and VEGF expression levels. The expression of HO-1 was not significantly altered as a result of high glucose treatment; however, it decreased following the downregulation of hsa_circ_0054633 expression (Fig. 2I-L).

Interaction between hsa_circ_0054633 and miR-218. Next, the study aimed to determine the interaction between miR-218

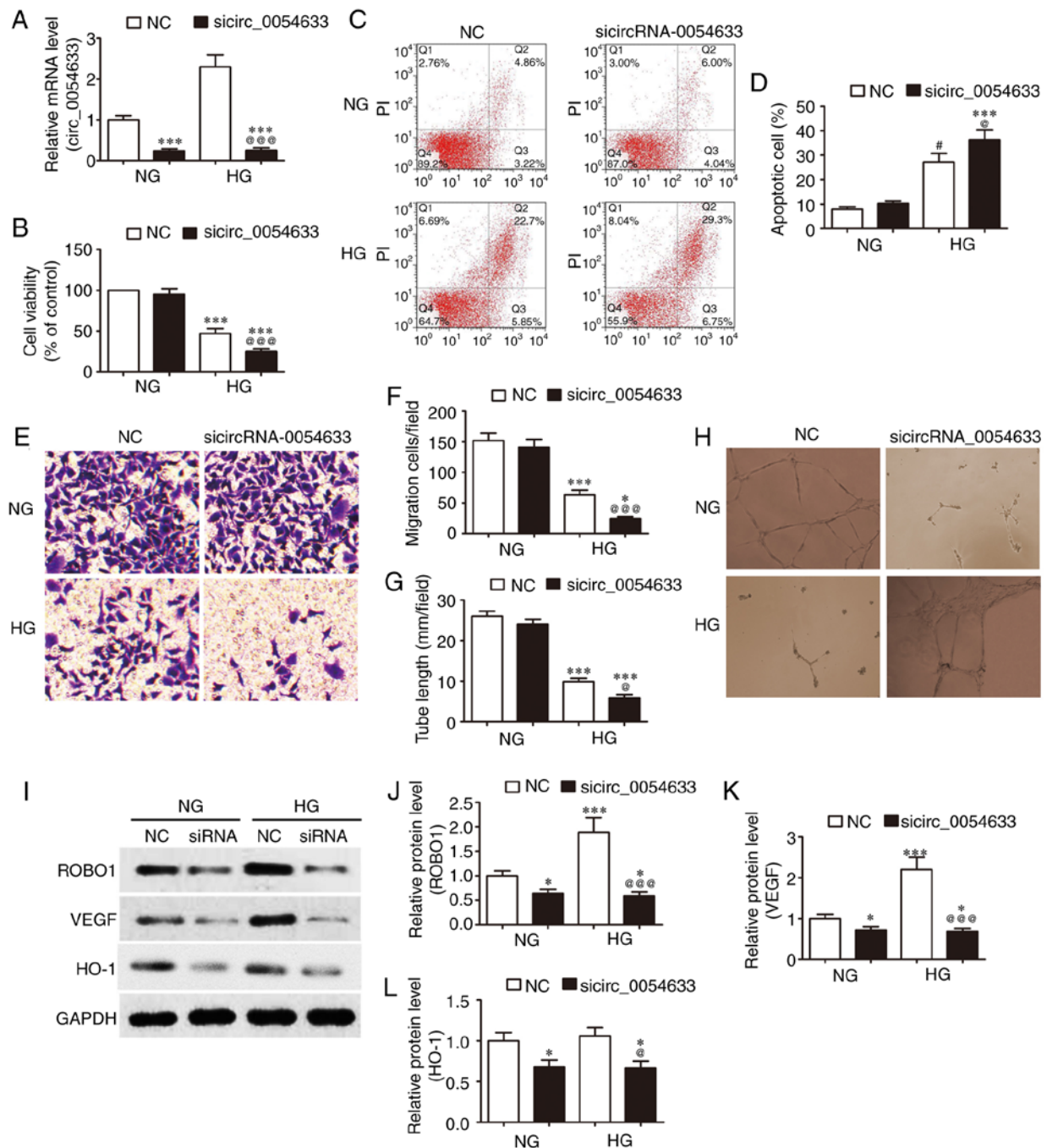


Figure 2. Downregulation of circRNA-0054633 expression increased the high glucose-induced endothelial cell dysfunction. HUVECs transfected with/without siRNA against hsa_circ_0054633 were treated with a normal (5.5 mM) or high (33 mM) concentration of glucose for 48 h. (A) hsa_circ_0054633 expression was analyzed by reverse transcription-quantitative polymerase chain reaction. (B) Cell viability was detected by a cell counting kit-8 assay after 48 h. (C) Flow cytometry graphs and (D) apoptotic cell percentage of HUVECs stained with Annexin-V-FITC/PI. (E) Crystal violet staining of migrating cells and (F) migration rate graph. Downregulating the expression of circRNA-0054633 aggravated the inhibitory effect of HG on the migration of HUVECs. (G) Effect of circRNA-0054633 on tube formation ability and (H) phase-contrast images. At 16 h after the addition of pretreated HUVECs to the Matrigel, images were acquired and analyzed in Image-Pro Plus for quantification of the tube length. (I) Western blots, and quantified protein expression levels of (J) ROBO1, (K) VEGF and (L) HO-1 in HUVECs. Data are represented as the mean \pm standard deviation. * P <0.05 and *** P <0.001 vs. NC + NG; # P <0.05 and @ P <0.001 vs. NC + HG. hsa_circ_0054633, human circular RNA-0054633; HUVECs, human umbilical vein endothelial cells; NC, normal control; NG, normal glucose; HG, high glucose; ROBO1, roundabout 1; HO-1, heme oxygenase-1; VEGF, vascular endothelial growth factor.

and hsa_circ_0054633. Initially, a bioinformatic comparison was performed between miR-218 and hsa_circ_0054633. Overlap analysis indicated that the binding sites of miR-218 were more broadly conserved to hsa_circ_0054633. A mutated version of hsa_circ_0054633 was generated, in which 10 complementary nucleotides in the binding site were

altered. This mutated construct was fused to the luciferase coding region and co-transfected into 293 cells along with miR-218 mimics (Fig. 3A). The results demonstrated that miR-218 expression in 293 cells was significantly increased subsequent to transfection with miR-218 mimics (Fig. 3B). Determination of the relative luciferase activity revealed that,

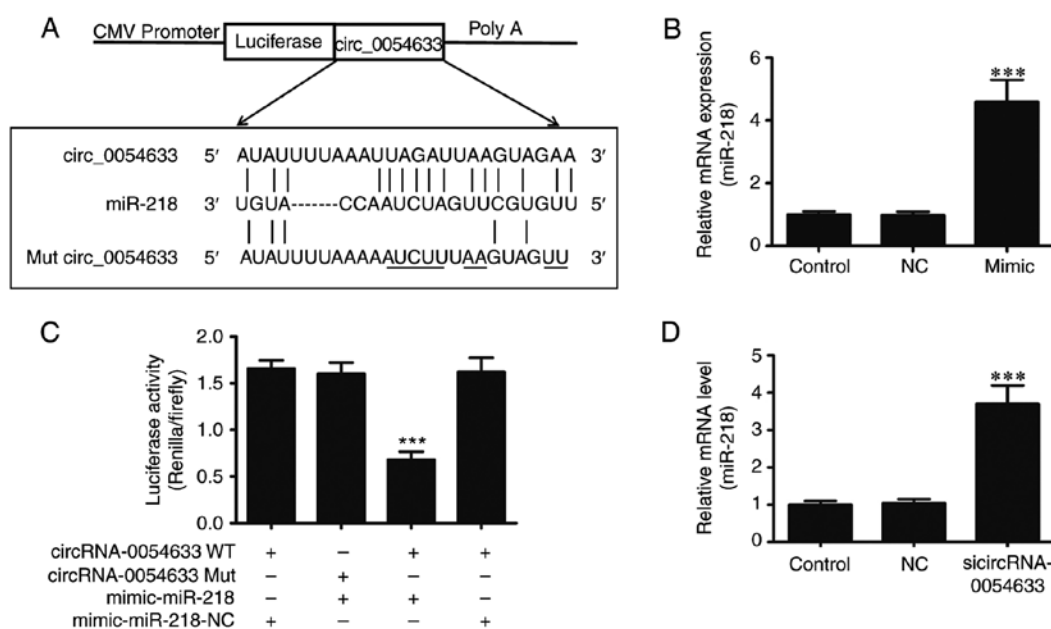


Figure 3. hsa_circ_0054633 is a target of miR-218. (A) Sequence alignment between miR-218 and hsa_circ_0054633. Complementary bases between the sequences are underlined. The sequence of the mutant circRNA-0054633 construct is also shown. (B) RT-qPCR detection demonstrated the expression of miR-218 in 293 cells following transfection with miR-218 mimics or NC, and in the untransfected control. (C) Dual-luciferase reporter assay of 293 cells co-transfected with circRNA-0054633-WT or circRNA-0054633-Mut, and with miR-218 mimic or miR-NC. (D) miR-218 expression in HUVECs was measured by RT-qPCR following transfection with siRNA against circRNA-0054633 for 48 h. The results revealed that downregulating the expression of circRNA-0054633 significantly increased miR-218 expression. Data are represented as the mean \pm standard deviation from six individual experiments. *** P <0.001 vs. control group. hsa_circ_0054633, human circular RNA-0054633; HUVECs, human umbilical vein endothelial cells; miR, microRNA; siRNA, small interfering RNA; RT-qPCR, reverse transcription-quantitative polymerase chain reaction; NC, normal control; WT, wild-type; Mut, mutated.

when the wild-type hsa_circ_0054633 was co-transfected with miR-218 mimics, hsa_circ_0054633 expression was significantly decreased compared with that upon co-transfection with control miRNA. However, this effect was not observed when the mutant hsa_circ_0054633 construct was used for co-transfection, indicating the specific targeting and suppression of miR-218 by hsa_circ_0054633 (Fig. 3C). Taken together, the dual-luciferase reporter analysis suggested that hsa_circ_0054633 interacted with miR-218. To further identify whether decreased hsa_circ_0054633 expression is able to remove this inhibitory effect, siRNA against hsa_circ_0054633 was transfected into HUVECs. RT-qPCR analysis demonstrated that decreased hsa_circ_0054633 expression significantly increased miR-218 expression, suggesting that the regulation effect of hsa_circ_0054633 on HUVEC proliferation, migration and angiogenesis is mediated by miR-218 (Fig. 3D).

Regulation effect of miR-218 on high glucose-induced endothelial cell dysfunction. To identify the effect of miR-218 on endothelial cell proliferation, migration and angiogenesis, HUVECs were pretreated with miR-218-specific inhibitors for 48 h. Next, the expression of miR-218 was measured by RT-qPCR. The results demonstrated that the expression of miR-218 was significantly decreased compared with the NC group (Fig. 4A). In order to identify the effect of miR-218 on high glucose-induced HUVEC proliferation, migration and angiogenesis, HUVECs pretreated with/without miR-218 inhibitor were co-treated with different concentrations of glucose (5.5 and 33 mM) for 48 h. Subsequently, the proliferation (Fig. 4B) and apoptosis (Fig. 4C and D) of HUVECs

were detected by CCK-8 assay and flow cytometry. The results identified that downregulation of the expression of miR-218 reversed the suppressive effect of high glucose on the proliferative activity and decreased the apoptotic ratio. In addition, the migration of HUVECs was detected by Transwell assay, and it was observed that downregulation of the expression of miR-218 suppressed the high glucose-induced migration (Fig. 4E and F). To further assess the angiogenic function of miR-218, an *in vitro* capillary tube formation assay was conducted. This assay indicated that high glucose treatment significantly suppressed the tube formation and that this phenomenon was reversed following downregulation of the expression of miR-218 (Fig. 4G and H). Western blot analysis also revealed that high glucose increased the expression levels of ROBO1 and VEGF, while the downregulation of miR-218 expression further increased these levels. By contrast, the expression of HO-1 was not significantly altered by high glucose treatment, whereas it increased subsequent to the downregulation of miR-218 expression (Fig. 4I-L).

Interaction of miR-218, HO-1, and ROBO1. Previous studies have demonstrated that miR-218 targets HO-1 and ROBO1, and that the expression of miR-218 promotes high glucose-induced cell apoptosis (17,18). Furthermore, the expression of HO-1 or ROBO1 promotes cell survival. In order to identify whether miR-218 regulates high glucose-induced endothelial dysfunction by targeting HO-1 and ROBO1, the TargetScan databases was used to search any potential interactions between miR-218 and the 3'-UTR of HO-1 or ROBO1. Subsequently, the wild-type and mutant 3'-UTR sequences of HO-1 and ROBO1 were cloned into

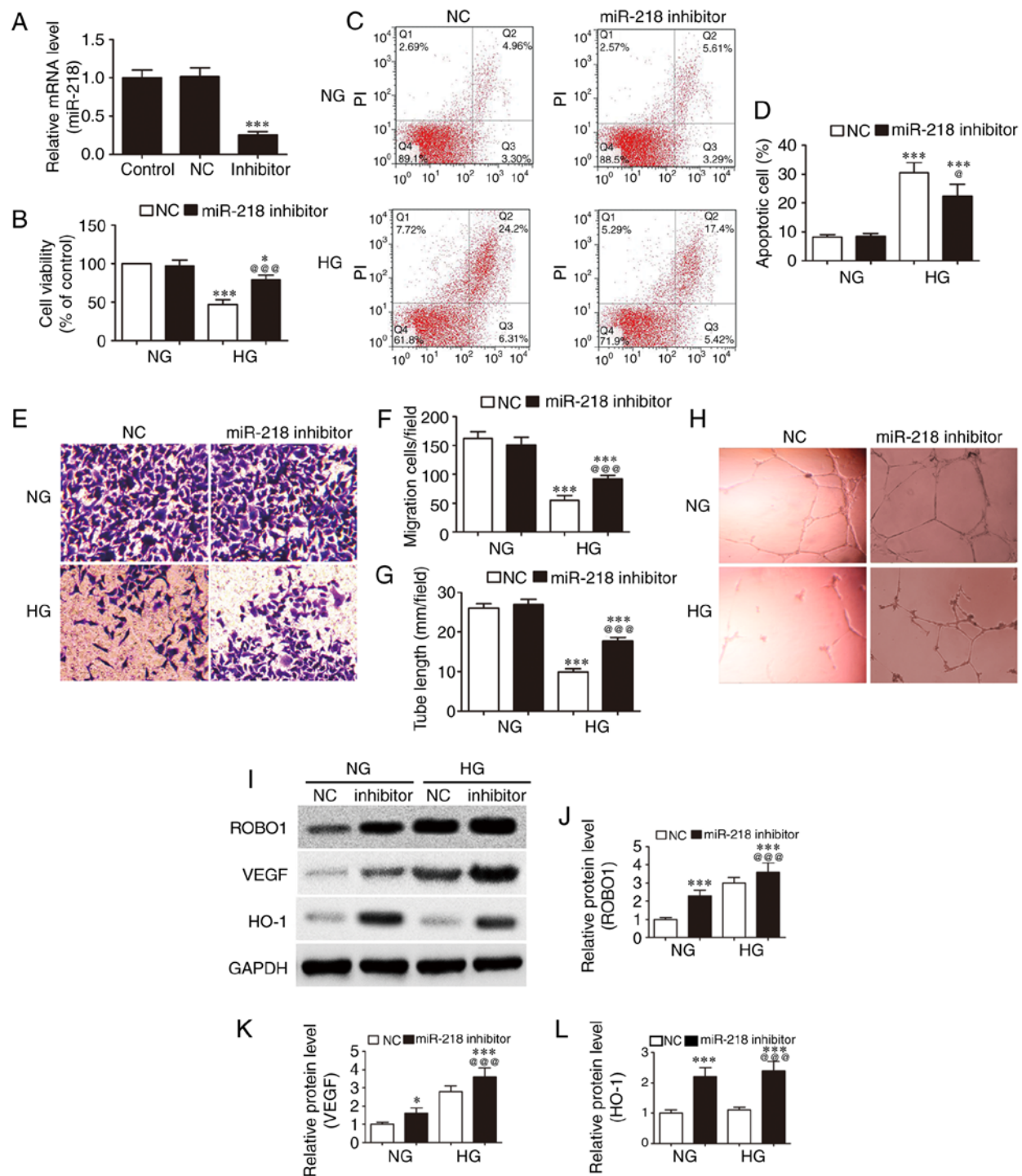


Figure 4. Downregulation of miR-218 expression inhibits the high glucose-induced endothelial cell dysfunction. HUVECs were treated with/without miR-218 inhibitor, followed by normal (5.5 mM) or high (33 mM) concentration of glucose for 48 h. (A) miR-218 expression was analyzed by reverse transcription-quantitative polymerase chain reaction. *** $P < 0.001$ vs. control group. (B) Cell viability was detected by cell counting kit-8 after 48 h. (C) Apoptotic percentage of HUVECs and (D) flow cytometry graphs. (E) Crystal violet staining of migrating cells and (F) migration rate, measured by a Transwell assay. (G) Effect of miR-218 on tube formation ability and (H) phase-contrast images. At 16 h after addition of pretreated HUVECs to the Matrigel, images were acquired and analyzed by Image-Pro Plus for quantification of the tube length. (I) Western blots, and quantified protein levels of (J) ROBO1, (K) VEGF and (L) HO-1. Data are represented as the mean \pm standard deviation. * $P < 0.05$ and *** $P < 0.001$ vs. NC + NG; @ $P < 0.05$ and @@@ $P < 0.001$ vs. NC + HG. HUVECs, human umbilical vein endothelial cells; NC, normal control; NG, normal glucose; HG, high glucose; ROBO1, roundabout 1; HO-1, heme oxygenase-1; VEGF, vascular endothelial growth factor.

luciferase reporter vectors (Fig. 5A and B). The luciferase assay revealed that miR-218 suppressed the luciferase activities of HO-1 and ROBO1 containing a wild-type 3'-UTR; however, it did not suppress the activities of ROBO1 and HO-1 containing a mutant 3'-UTR (Fig. 5C and D). RT-PCR

analysis also demonstrated that inhibiting miR-218 expression significantly increased the expression levels of ROBO1 and HO-1 (Fig. 5E and F). These findings suggested that miR-218 regulates the high glucose-induced endothelial dysfunction by targeting HO-1 and ROBO1.

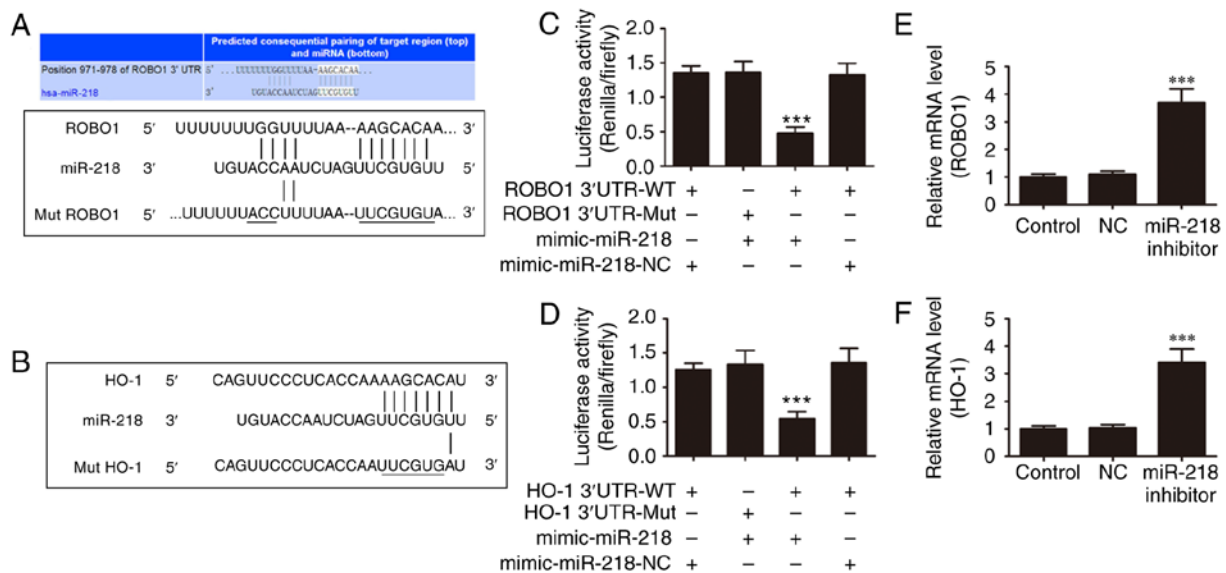


Figure 5. miR-218 targets ROBO1 and HO-1. (A) Sequence alignment between miR-218 and the 3'-UTR of human ROBO1. Complementary bases between the sequences are shown as underlined. The sequence of the mutant ROBO1 construct is also shown. (B) Sequence alignment between miR-218 and the 3'-UTR of human HO-1. Complementary bases between the sequences are underlined. The sequence of the mutant HO-1 construct is also shown. (C) Dual-luciferase reporter assay of 293 cells co-transfected with ROBO1 3'-UTR-WT or 3'-UTR-Mut, and with miR-218 mimic or miR-NC. (D) Dual-luciferase reporter assay of 293 cells co-transfected with HO-1 3'-UTR-WT or 3'-UTR-Mut, and with miR-218 mimic or miR-NC. (E) RT-qPCR was used to analyze the mRNA expression of ROBO1 in HUVECs following treatment with miR-218 inhibitor for 48 h. (F) RT-qPCR analysis was performed to examine the mRNA expression of HO-1 in HUVECs following treatment with miR-218 inhibitor for 48 h. Data are represented as the mean \pm standard deviation. *** $P < 0.001$ vs. control group. miR, microRNA; ROBO1, roundabout 1; HO-1, heme oxygenase-1; HUVECs, human umbilical vein endothelial cells; RT-qPCR, reverse transcription-quantitative polymerase chain reaction; UTR, untranslated region; NC, normal control; WT, wild-type; Mut, mutated.

Discussion

The expression of circRNAs in plants has been well established for decades, thus, these are not a novel RNA subtype (24). However, in spite of increasing knowledge, in-depth details on the functions of circRNAs in multiple human diseases remain poorly understood, particularly in diabetic angiopathy. Numerous circRNAs have been identified to be involved in a regulation effect in stress environments, including the circRNAs cZNF292, cAFF1 and cDENND4C (25). Vascular endothelial cell (VEC) dysfunction is considered pivotal to pathogenesis and the initial step for a series of CVDs, including atherosclerosis, thrombus formation, hypertension and diabetic cardiovascular complications (26). Thus, the functional study of VECs is critical for the identification of novel therapies for CVD (27). However, the role of circRNAs in VEC function remains to be elucidated. Previously, hsa_circ_0054633 expression was observed to be significantly increased in T2DM, following the analysis of the circRNA expression profiles in this disease. This suggests that hsa_circ_0054633 may present a certain diagnostic capability for pre-diabetes and T2DM (12). However, the potential regulatory mechanism of circRNAs in high glucose-induced HUVECs remains unclear.

circRNAs, a family of naturally occurring endogenous noncoding RNAs, has been reported to have diverse functions and widespread distribution. circRNAs are single-stranded RNA molecules with a length of ~100 nucleotides that form a circle through covalent binding (28-30). They are highly represented in the eukaryotic transcriptome, while they are also abundant in exosomes. A large number of circRNAs have been identified to date, while certain circRNAs have been

confirmed to function as miRNA sponges in mammalian cells through bioinformatics analysis and high-throughput RNA sequencing (29-31). In addition, a previous study has demonstrated that circRNAs function as an miRNA sponge that can mediated cell metabolism (32).

In the present study, bioinformatics analysis identified that hsa_circ_0054633 targets miR-218, and this was then verified by dual-luciferase analysis. The study then further assessed whether hsa_circ_0054633 is able to function as an miR-218 sponge to regulate the circRNA-miRNA-mRNA network. hsa_circ_0054633 expression was knocked down in HUVECs, and the results revealed that downregulation of hsa_circ_0054633 expression significantly increased miR-218 expression. The present study also demonstrated that hsa_circ_0054633 expression in HUVECs was increased following exposure to high glucose. In addition, hsa_circ_0054633 expression suppressed the injury effects of high glucose to HUVECs by targeting miR-218. Numerous studies have illustrated that the expression of miR-218 inhibits the cell proliferation, migration and angiogenesis (20,33-38). The current study also identified that the expression of miR-218 was able to inhibit the high glucose-induced HUVEC proliferation, migration and angiogenesis by targeting ROBO1 and HO-1. A previous study verified that the high expression levels of ROBO1 and HO-1 were able to significantly increase cell migration, proliferation and angiogenesis (17,18,39). Herein, it was also observed that the expression of VEGF was increased in high glucose conditions. However, angiogenesis was suppressed upon decreased hsa_circ_0054633 expression in normal conditions, whereas overexpression of hsa_circ_0054633 or inhibition of miR-218 increased angiogenesis. These observations suggested that the overexpression of hsa_circ_0054633 increased HO-1

expression by targeting miR-218, which resulted in eventually reducing the apoptosis of HUVECs. There is already evidence showing that VEGF receptor 2 becomes inactive and no longer responds to VEGF stimulation with the increase of cellular H₂O₂ (32), which indicates that hsa_circ_0054633 expression may also suppress cellular oxidative stress.

In conclusion, the present study observed that high glucose treatment was able to induce the increase of hsa_circ_0054633 and miR-218 expression levels. However, increased hsa_circ_0054633 expression was unable to entirely inhibit miR-218 expression. Furthermore, overexpression of hsa_circ_0054633 may effectively reverse high glucose-induced cell proliferation, migration and angiogenesis inhibition by targeting the miR-218/ROBO1 and miR-218/HO-1 signals.

Acknowledgements

Not applicable.

Funding

No funding was received.

Availability of data and materials

All data generated or analyzed during this study are included in this published article.

Author's contributions

XL, LP, WL and SH generated and analyzed the data. CC, XZ and ML designed the experiments and drafted the manuscript. All authors approved the final version of the manuscript.

Ethics approval and consent to participate

Not applicable.

Consent for publication

Not applicable.

Competing interests

The authors declare that they have no competing interests.

References

- Zatalia SR and Sanusi H: The role of antioxidants in the pathophysiology, complications, and management of diabetes mellitus. *Acta Med Indones* 45: 141-147, 2013.
- Ghassemi H, Harrison G and Mohammad K: An accelerated nutrition transition in Iran. *Public Health Nutr* 5: 149-155, 2002.
- Hossain P, Kavar B and El Nahas M: Obesity and diabetes in the developing world-a growing challenge. *N Engl J Med* 356: 213-215, 2007.
- Huxley R, Barzi F and Woodward M: Excess risk of fatal coronary heart disease associated with diabetes in men and women: Meta-analysis of 37 prospective cohort studies. *BMJ* 332: 73-78, 2006.
- McFarlane SI, Salifu MO, Makaryus J and Sowers JR: Anemia and cardiovascular disease in diabetic nephropathy. *Curr Diab Rep* 6: 213-218, 2006.
- Seetharam D, Mineo C, Gormley AK, Gibson LL, Vongpatanasin W, Chambliss KL, Hahner LD, Cummings ML, Kitchens RL, Marcel YL, *et al*: High-density lipoprotein promotes endothelial cell migration and reendothelialization via scavenger receptor-B type I. *Circ Res* 98: 63-72, 2006.
- Li Y, Zhao M, He D, Zhao X, Zhang W, Wei L, Huang E, Ji L, Zhang M, Willard B, *et al*: HDL in diabetic nephropathy has less effect in endothelial repairing than diabetes without complications. *Lipids Health Dis* 15: 76, 2016.
- Shang C, Lang B, Ao CN and Meng L: Long non-coding RNA tumor suppressor candidate 7 advances chemotherapy sensitivity of endometrial carcinoma through targeted silencing of miR-23b. *Tumour Biol* 39: 1010428317707883, 2017.
- Iparraguirre L, Muñoz-Culla M, Prada-Luengo I, Castillo-Triviño T, Olascoaga J and Otaegui D: Circular RNA profiling reveals that circular RNAs from ANXA2 can be used as new biomarkers for multiple sclerosis. *Hum Mol Genet* 26: 3564-3572, 2017.
- Yao T, Chen Q, Fu L and Guo J: Circular RNAs: Biogenesis, properties, roles, and their relationships with liver diseases. *Hepatol Res* 47: 497-504, 2017.
- Hou LD and Zhang J: Circular RNAs: An emerging type of RNA in cancer. *Int J Immunopathol Pharmacol* 30: 1-6, 2017.
- Zhao Z, Li X, Jian D, Hao P, Rao L and Li M: Hsa_circ_0054633 in peripheral blood can be used as a diagnostic biomarker of pre-diabetes and type 2 diabetes mellitus. *Acta Diabetol* 54: 237-245, 2017.
- Yan B, Yao J, Liu JY, Li XM, Wang XQ, Li YJ, Tao ZF, Song YC, Chen Q and Jiang Q: lncRNA-MIAT regulates microvascular dysfunction by functioning as a competing endogenous RNA. *Circ Res* 116: 1143-1156, 2015.
- Li X, Zeng L, Cao C, Lu C, Lian W, Han J, Zhang X, Zhang J, Tang T and Li M: Long noncoding RNA MALAT1 regulates renal tubular epithelial pyroptosis by modulated miR-23c targeting of ELAVL1 in diabetic nephropathy. *Exp Cell Res* 350: 327-335, 2017.
- Kumar L, Shamsuzzama, Haque R, Baghel T and Nazir A: Circular RNAs: The emerging class of non-coding RNAs and their potential role in human neurodegenerative diseases. *Mol Neurobiol* 54: 7224-7234, 2016.
- Kulcheski FR, Christoff AP and Margis R: Circular RNAs are miRNA sponges and can be used as a new class of biomarker. *J Biotechnol* 238: 42-51, 2016.
- Yang H, Wang Q and Li S: microRNA-218 promotes high glucose-induced apoptosis in podocytes by targeting heme oxygenase-1. *Biochem Biophys Res Commun* 471: 582-588, 2016.
- Zhang X, Dong J, He Y, Zhao M, Liu Z, Wang N, Jiang M, Zhang Z, Liu G and Liu H, *et al*: miR-218 inhibited tumor angiogenesis by targeting ROBO1 in gastric cancer. *Gene* 615: 42-49, 2017.
- Wang J, Zhou Y, Fei X, Chen X, Chen R, Zhu Z and Chen Y: Integrative bioinformatics analysis identifies ROBO1 as a potential therapeutic target modified by miR-218 in hepatocellular carcinoma. *Oncotarget* 8: 61327-61337, 2017.
- Fang M, Du H, Han B, Xia G, Shi X, Zhang F, Fu Q and Zhang T: Hypoxia-inducible microRNA-218 inhibits trophoblast invasion by targeting LASP1: Implications for preeclampsia development. *Int J Biochem Cell Biol* 87: 95-103, 2017.
- Mahmoud AM, Zaki AR, Hassan ME and Mostafa-Hedeab G: *Commiphora molmol* resin attenuates diethylnitrosamine/phenobarbital-induced hepatocarcinogenesis by modulating oxidative stress, inflammation, angiogenesis and Nrf2/ARE/HO-1 signaling. *Chem Biol Interact* 270: 41-50, 2017.
- Zhong ZY and Tang Y: Upregulation of periostin prevents high glucose-induced mitochondrial apoptosis in human umbilical vein endothelial cells via activation of Nrf2/HO-1 signaling. *Cell Physiol Biochem* 39: 71-80, 2016.
- Livak KJ and Schmittgen TD: Analysis of relative gene expression data using real-time quantitative PCR and the 2^{-ΔΔCT} method. *Methods* 25: 402-408, 2001.
- Szabo L and Salzman J: Detecting circular RNAs: Bioinformatic and experimental challenges. *Nat Rev Genet* 17: 679-692, 2016.
- Boeckel JN, Jaé N, Heumüller AW, Chen W, Boon RA, Stellos K, Zeiher AM, John D, Uchida S and Dimmeler S: Identification and characterization of hypoxia-regulated endothelial circular RNA. *Circ Res* 117: 884-890, 2015.
- Shin HJ, Kim SN, Chung H, Kim TE and Kim HC: Intravitreal anti-vascular endothelial growth factor therapy and retinal nerve fiber layer loss in eyes with age-related macular degeneration: A meta-analysis. *Invest Ophthalmol Vis Sci* 57: 1798-1806, 2016.

27. Aragona CO, Imbalzano E, Mamone F, Cairo V, Lo Gullo A, D'Ascola A, Sardo MA, Scuruchi M, Basile G, Saitta A and Mandraffino G: Endothelial progenitor cells for diagnosis and prognosis in cardiovascular disease. *Stem Cells Int* 2016: 8043792, 2016.
28. Memczak S, Jens M, Elefsinioti A, Torti F, Krueger J, Rybak A, Maier L, Mackowiak SD, Gregersen LH, Munschauer M, *et al*: Circular RNAs are a large class of animal RNAs with regulatory potency. *Nature* 495: 333-338, 2013.
29. Chen LL and Yang L: Regulation of circRNA biogenesis. *RNA Biol* 12: 381-388, 2015.
30. Chen I, Chen CY and Chuang TJ: Biogenesis, identification, and function of exonic circular RNAs. *Wiley Interdiscip Rev RNA* 6: 563-579, 2015.
31. Lu D and Xu AD: Mini review: Circular RNAs as potential clinical biomarkers for disorders in the central nervous system. *Front Genet* 7: 53, 2016.
32. Kang DH, Lee DJ, Lee KW, Park YS, Lee JY, Lee SH, Koh YJ, Koh GY, Choi C, Yu DY, *et al*: Peroxiredoxin II is an essential antioxidant enzyme that prevents the oxidative inactivation of VEGF receptor-2 in vascular endothelial cells. *Mol Cell* 44: 545-558, 2011.
33. Zeng XJ, Wu YH, Luo M, Cong PG and Yu H: Inhibition of pulmonary carcinoma proliferation or metastasis of miR-218 via down-regulating CDCP1 expression. *Eur Rev Med Pharmacol Sci* 21: 1502-1508, 2017.
34. Shi ZM, Wang L, Shen H, Jiang CF, Ge X, Li DM, Wen YY, Sun HR, Pan MH, Li W, *et al*: Downregulation of miR-218 contributes to epithelial-mesenchymal transition and tumor metastasis in lung cancer by targeting Slug/ZEB2 signaling. *Oncogene* 36: 2577-2588, 2017.
35. Wang LL, Wang L, Wang XY, Shang D, Yin SJ, Sun LL and Ji HB: microRNA-218 inhibits the proliferation, migration, and invasion and promotes apoptosis of gastric cancer cells by targeting LASP1. *Tumour Biol* 37: 15241-15252, 2016.
36. Han S, Kong YC, Sun B, Han QH, Chen Y and Wang YC: microRNA-218 inhibits oxygen-induced retinal neovascularization via reducing the expression of roundabout 1. *Chin Med J* 129: 709-715, 2016.
37. Kong Y, Sun B, Han Q, Han S, Wang Y and Chen Y: Slit-miR-218-Robo axis regulates retinal neovascularization. *Int J Mol Med* 38: 1947, 2016.
38. Amin ND, Bai G, Klug JR, Bonanomi D, Pankratz MT, Gifford WD, Hinckley CA, Sternfeld MJ, Driscoll SP, Dominguez B, *et al*: Loss of motoneuron-specific microRNA-218 causes systemic neuromuscular failure. *Science* 350: 1525-1529, 2015.
39. Guerrero-Cazares H, Lavell E, Chen L, Schiapparelli P, Lara-Velazquez M, Capilla-Gonzalez V, Clements AC, Drummond G, Noiman L, Thaler K, *et al*: Brief report: Robo1 regulates the migration of human subventricular zone neural progenitor cells during development. *Stem Cells* 35: 1860-1865, 2017.